

Measurement of plaque-forming macrophages activated by lipopolysaccharide in a micro-channel chip

T. Isoda¹, T. Tsutsumi²,
K. Yamazaki¹, T. Nishihara²

¹Department of Life and Environment Engineering, Faculty of Environmental Engineering, University of Kitakyushu, 1-1, Hibikino, Wakamatsu, Kitakyushu, 808-0135, Japan and ²Division of Infections and Molecular Biology, Department of Health Promotion, Kyushu Dental College, 2-6-1, Manazuru, Kokurakita, Kitakyushu, 808-8580, Japan

Isoda T, Tsutsumi T, Yamazaki K, Nishihara T. Measurement of plaque-forming macrophages activated by lipopolysaccharide in a micro-channel chip. *J Periodont Res* 2009; 44: 609–615. © 2009 The Authors. Journal compilation © 2009 Blackwell Munksgaard

Background and Objective: In the present study, micro-channel arrays were fabricated on the surface of plastic-based disposable chips. The cell adhesion process and the detection of plaque-forming macrophages were observed. Further, we evaluated cell adhesion in a fluid system *in vitro*.

Material and Methods: Features of the micro-channel (1.4 mm wide and 10 mm long) included twenty micro-pillars (with a projection of 200 µm diameter and 250 µm high) coated in a 50 µm thick silicon rubber layer, which were regularly arranged at the bottom of each channel. The efficiency of cell capture was expected to increase by arrangement of micro-pillars in a micro-channel. Mouse macrophage RAW264.7 cells, stimulated for 24 h with lipopolysaccharide (LPS) derived from periodontopathic bacteria, were circulated continuously for 2 h at room temperature by the pump in a chip.

Results: Control cells had not formed plaques on micro-pillars 20 min into the experiment. By contrast, LPS-activated macrophages produced plaques at the side walls of micro-pillars after 20 min. The plaques grew during the flow test, and image shading became clearer with increasing flow time for 120 min. The maximal adhesion rate per unit area appeared at 20% for control cells, whereas the peak was shifted to 30% for LPS-activated macrophages ($n = 20$). The average adhesion rate was $3.0 \pm 2.0\%$ for control cells and $5.0 \pm 3.9\%$ for LPS-activated macrophages ($n = 100$).

Conclusion: These findings indicate that LPS-activated macrophages accumulate in micro-channel arrays, and suggest that macrophage plaque formation is a two-step procedure: (1) LPS-activated macrophages adhere physically to the silicon rubber layer on micro-pillars; and (2) consequently, the cells adhere to the activated macrophage layer.

Takaaki Isoda, PhD, Department of Life and Environment Engineering, Faculty of Environmental Engineering, University of Kitakyushu, 1-1, Hibikino, Wakamatsu, Kitakyushu, 808-0135, Japan
Tel: +81 93 695 3285
Fax: +81 93 695 3377
e-mail: isoda@env.kitakyu-u.ac.jp

Key words: periodontopathic bacteria; cell adhesion; atherosclerosis; macrophage

Accepted for publication August 12, 2008

Recently, an association between periodontal diseases and myocardial infarction was noted during epidemiological investigations. For example, one pathogen in periodontitis,

Aggregatibacter actinomycetemcomitans, has been detected in cardiovascular tissues (1). It has been reported that the distribution of *A. actinomycetemcomitans* in specimens of 106 car-

diovascular and dental plaque samples was analysed using a polymerase chain reaction method, which resulted in a positive reaction in 33 (31.1%) of the cardiovascular specimens and 25

(46.3%) of the dental plaque samples (1). However, neither the mechanism nor the causal association has been clarified.

There have been many *in vitro* studies on the possible involvement of periodontopathic bacteria in the development of atherosclerosis. It has been reported that *Porphyromonas gingivalis* could induce macrophages to form foam cells (2). Infection of macrophages with increasing numbers of *P. gingivalis* resulted in higher levels of foam cell formation. In this case, more than 70% of the cultured macrophages were changed into a cell included in a droplet of cholesterol ester when 100 µg/mL of low-density lipoprotein (LDL) was added to a culture containing 10 bacteria per cell.

The atherogenic properties of lipopolysaccharide (LPS) derived from *A. actinomycetemcomitans* (LPS-*A.a.*), serotypes b and d strains, have also been investigated on macrophages (RAW264.7 cells; 3). The LPS-*A.a.* was found to induce foam cell formation and cholesteryl ester (CE) accumulation from native LDL, and LPS-*A.a.* from strain JP2 (serotype b) had a higher activity than strain Y4 (serotype b) and IDH781 (serotype d).

The LPS concentration is well known to correlate positively with the serum concentration of LDL and oxidized LDL (oxLDL), resulting in an increase of LDL-CE uptake and production of cytokines (4). Baranova *et al.* (5) further investigated the mechanism of LPS-induced cholesterol accumulation at the level of gene expression, and reported that LPS down-regulated both scavenger receptor B1 and ATP binding cassette transporter A1 in RAW264.7 cells. The effect of gene expression in macrophages previously exposed to oxLDL was also clarified (6). In this case, LPS enhanced gene expression of tumor necrosis factor (TNF) and interleukin-6 (IL-6) in macrophages (6), whereas expression of the anti-inflammatory cytokine IL-10 and interferon-β was decreased in foam cells (6). Although atherosclerosis is known to be a complex pathological process initiated by the formation of cholesterol-rich plaque, the precise mechanism by which

periodontopathic bacterial LPS causes arteriosclerosis to develop is not clear because the plaque formation process has not yet been observed directly *in vivo* or *in vitro*. It is necessary to establish an observation procedure for the aggregation process of macrophages (plaque formation) in a pseudo-vessel system.

In this study, micro-channel arrays were fabricated on the surface of a plastic-based disposable chip, and both the cell adhesion process and plaque formation were observed. The evaluation of cell adhesion in a fluid system was also examined. The main focus of this study was to establish a method for measuring the difference in adhesion between control and LPS-activated macrophages within a micro-channel chip. The plaque formation process of LPS-activated cells in a fluid is discussed.

Material and methods

Fabrication of a micro-channel chip

Figure 1 shows the fabrication process. The fabrication pattern was designed using CAD software (Roland DG Co., Shizuoka, Japan), and the patterning was carried out using an automatic drilling system. A mold structure of 250 µm depth was patterned onto the surface of an acrylic resin board (1 mm thick, Sumitomo Chemical, Inc., Tokyo, Japan) and was coated with fluorinated resin as a removal agent (Fig. 1A). Micro-pillar structures (200 µm diameter and 250 µm high) located in a channel (250 µm deep × 1.4 mm wide) were also fabricated onto the surface of an acrylic resin board (Fig. 1B). Silicon rubber filler (Sumitomo 3M, Ltd, Tokyo, Japan) was sandwiched between the

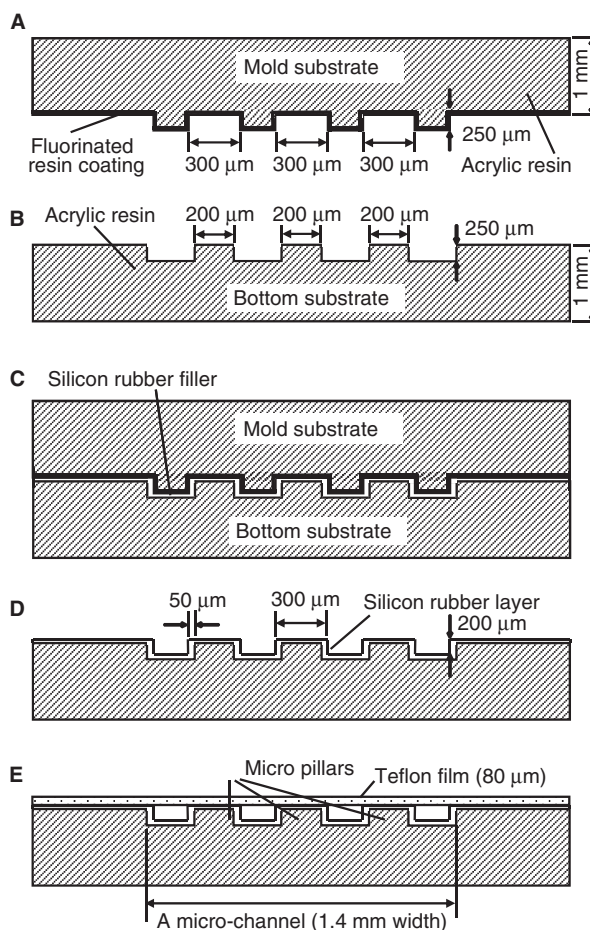


Fig. 1. Steps in the fabrication of the micro-channel chip (shown as cross-section A–B in Fig. 2).

mold substrate and the bottom substrate (Fig. 1C). After fixing the silicon rubber filler, the mold substrate was removed so that the wall side of a micro-pillar was coated with a silicon rubber layer 50 μm thick (Fig. 1D). A Teflon film layer was used as an upper substrate (80 μm , polytetrafluoroethylene tape; Sumitomo 3M, Ltd) and was fixed on the bottom substrate (Fig. 1E).

Figure 2 shows photographs of a micro-channel chip. Liquid samples were injected into the chip at the entrance (Fig. 2B, a) through a tube (2 mm diameter) attached to the chip. A reservoir was filled with the liquid sample (Fig. 2B, b), and the liquid flowed into each fluidic path (Fig. 2B, 1–5). Five paths (10 mm long and 1.4 mm wide) were formed on the bottom substrate, and a variety of arrangements of micro-pillars were located in each channel (Fig. 2B, c). The liquid sample was passed through each channel exit (Fig. 2B, 1'–5') and was collected in a reservoir. Finally, the liquid sample was removed at an exit (Fig. 2B, d) through a tube attached to the chip.

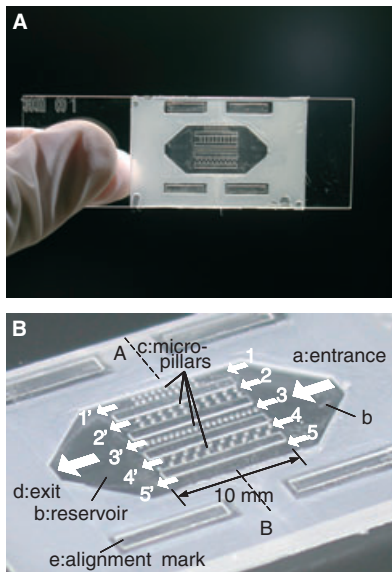


Fig. 2. Photographs of a micro-channel chip: overview image (A) and magnified image of channels (B). In (B), dashed line A–B indicated the position of the cross-section illustrated in Fig. 1. Lower case letters in (B) are as follows: a, entrance; b, reservoir; c, micro-pillars; d, exit; and e, alignment mark.

The arrangement of micro-pillars in a micro-channel is summarized in Table 1. There were twenty micro-pillars in a micro-channel. In the case of type 1, the D1 value (distance between the side wall of the pillar and the micro-channel wall) was changed from 250 to 550 μm , whereas the D2 value (distance between the side walls of two pillars) was fixed at 200 μm . The positions of micro-pillars were designed so that the arrangement of micro-pillars in a channel was zig-zagged with increasing channel number. In the case of type 2, micro-pillars were positioned so that the arrangement of micro-pillars in a channel was crowded with increasing channel number. The type 3 chip was designed so that micro-pillars in a channel were arranged in the same way as micro-channel no. 5 in the type 1 chip. There were 100 micro-channels per chip in the type 3 chip.

Flow test using macrophages in the micro-channel chip

Figure 3 shows a schematic illustration of a flow system. A chip was placed on the stage of an optical microscope and was connected to the reservoir containing sample solution and a peristaltic pump with a tube (2 mm diameter). The sample solution was circulated continuously with a magnetic stirrer for 2 h at room temperature by a pump in the chip. Images of macrophages attached to micro-pillars in the channels were taken using a CCD camera attached to the optical microscope and equipped with a computer.

Mouse-derived macrophage RAW-246.7 cells were grown in α -minimal essential medium (Gibco BRL, Grand Island, NY, USA) containing 5% heat-treated fetal calf serum, 100 units/mL penicillin G and 100 $\mu\text{g}/\text{mL}$ streptomycin under environmental conditions (control cells; –LPS cells). Another batch of control cells were cultured in a cell culture medium with 5% fetal calf serum and 1 $\mu\text{g}/\text{mL}$ LPS derived from *A. actinomycetemcomitans* Y4 at 37°C in an atmosphere of 5% CO_2 in air, in accordance with Nishihara *et al.* (7; LPS-stimulated cells; +LPS cells). Purification of LPS has been described

previously (8,9), and these reports showed that the composition was 41% neutral sugar, 8% hexosamine, 31% fatty acid, 2% protein and 2% phosphorus. Before the flow test, each sample of culture medium was prepared so that it contained 1.5×10^6 cells/mL. Each flow test used of 3 mL of the solution. The flow rate at the exit of a chip (Fig. 2B, d) was 5 mL/min, and the flow test was evaluated after 2 h at room temperature.

Analysis of plaque-forming macrophages

Figure 4 shows a schematic illustration of plaque-forming macrophages in a micro-channel chip. The side wall of a micro-pillar, where there was an impact area with the liquid stream and plaque formation, was defined as an analysis area (indicated as dotted rectangles in Fig. 4A).

After the flow test, pictures of each analysis area were taken at 100 points with a microscope.

Figure 4B depicts a definition for deconvolution of the plaque attached to a micro-pillar. The adhesion area of the plaque was obtained using image analysis software (DP2-BSW, Olympus Co., Tokyo, Japan). The adhesion rate of plaque-forming macrophages attached to a micro-pillar per unit area is defined in equation 1:

$$\begin{aligned} \text{Adhesion rate of plaque-forming} \\ \text{macrophages} (\% / 9 \times 10^4 \mu\text{m}^2) \\ = 100 \times Sc / (Su - 0.5 \times Sp) \quad (1) \end{aligned}$$

where Sc (μm^2) is the adhesion area of plaque-forming macrophages obtained by imaging analysis, Su ($250 \mu\text{m} \times 500 \mu\text{m}$) is the analysis area and Sp [$\pi \times (150 \mu\text{m})^2 \mu\text{m}^2$] is the area of a micro-pillar.

Results

Plaque formation of macrophages activated by LPS in a micro-channel chip

Figure 5 shows examples of optical microscope images where –LPS and/or +LPS cells are forming plaques attached to a micro-pillar during the flow test. A type 3 micro-channel chip

Table 1. Arrangement of micro-pillars in a micro-channel chip

Chip	Micro-channel no.	Number of micro-pillars	Position of micro-pillars			
			D1 [μm]	D2 [μm]	D3 [μm]	External view
Type 1	1 ^a	20	550	200	–	
Type 1	2 ^a	20	480	200	220	
Type 1	3 ^a	20	400	200	280	
Type 1	4 ^a	20	330	200	370	
Type 1	5 ^a	20	250	200	480	
Type 2	1 ^b	0	–	–	–	
Type 2	2 ^b	20	550	200	–	
Type 2	3 ^b	20	250	200	480	
Type 2	4 ^b	20	265	200	–	
Type 2	5 ^b	20	265	100	–	
Type 3	1-5 ^c	20 × 5 channels	250	200	480	

^aNumbers 1–5 of micro-channels were mounted on the same type 1 chip.

^bNumbers 1–5 of micro-channels were mounted on the same type 2 chip.

^cSame arrangement of type 1 chip of micro-channel no. 5.

(channel no. 5) was used, as shown in Table 1. In Fig. 5, the left- and right-side photographs show –LPS and +LPS cells, respectively. The times during the flow test at which the images were obtained are 0 (Fig. 5A1,B1), 20 (Fig. 5A2,B2), 60 (Fig. 5A3,B3) and 120 min (Fig. 5A4,B4). The flow direction of the sample solution was

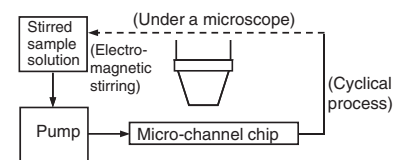


Fig. 3. Schematic illustration of a flow system.

left to right on each image view. Consequently, the liquid stream was constantly impacting against the left side of a micro-pillar.

There were no plaques containing –LPS cells on the left side of the micro-pillars at 0 (Fig. 5A1) and 20 min (Fig. 5A2). An hour later (Fig. 5A3), adhesion of cells had started, and plaque formation was observed for 120 min (Fig. 5A4). In contrast to –LPS cells, distinct plaque images of +LPS cells were observed on the left side of micro-pillars after the initial 20 min (Fig. 5B2). The plaque grew during the flow test, and the shade became clearer with increasing flow time at 60 (Fig. 5B3) and 120 min (Fig. 5B4). This suggests that aggre-

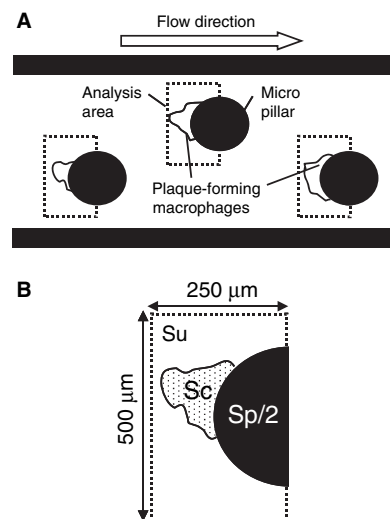


Fig. 4. Schematic illustration of plaque-forming macrophages in a micro-channel chip: top view (A) and a definition for deconvolution of the plaque attached to a micro-pillar (B). Abbreviations in (B): Su, analysis area ($250 \mu\text{m} \times 500 \mu\text{m}$); Sc, adhesion area of plaque-forming macrophages (μm^2); and Sp, area of micro-pillar [$\pi \times (150 \mu\text{m})^2$].

gation of +LPS cells progresses rapidly at the surface of the micro-pillar. As a result, a rigid plaque containing a high-density cell aggregate is formed.

Measurement of plaque formation by macrophages

Figure 6 shows the distributions of cell adhesion rate of –LPS cells (dotted lines) and +LPS cells (continuous lines). The cell adhesion rate is the rate of formation of an occupied area of a plaque per $S_u - 0.5 \times S_p$ area ($9.0 \times 10^4 \mu\text{m}^2$) as shown in Fig. 4B. Each sample solution was allowed to flow in micro-channels no. 1–5, within the type 1 chip and/or the type 3 chip, as shown in Table 1, for 2 h.

Figure 6A and B shows the typical distributions of adhesion rate of plaque-forming macrophages within micro-channels no. 4 and 5, respectively. Micro-pillars were arranged within a channel where the pillars approached the channel wall side further into the channel. As a result, pillar positioning was in a zigzag arrangement. With micro-channel no. 4, the

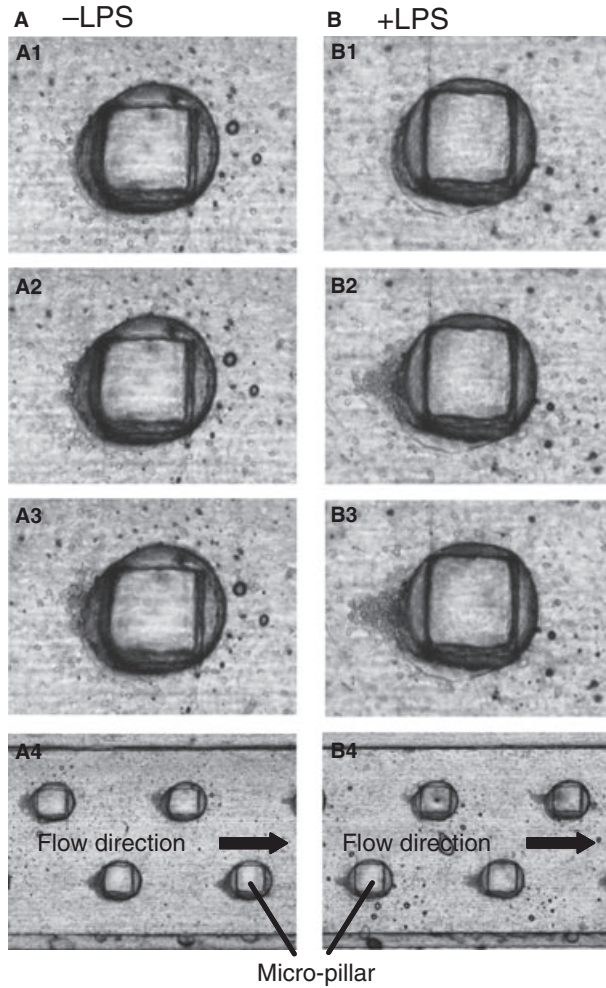


Fig. 5. Optical microscope images of plaque-forming macrophages attached to a micro-pillar in a micro-channel chip. Magnification of photographs: $\times 10$ (Figs. 5 A4 and B4) and $\times 27$ (other photographs). Left-side photographs (A1–A4) show control cells (–LPS) and right-side photographs (B1–B4) show cells activated by LPS (+LPS). A micro-channel chip (type 3 as shown in Table 1) was used. Time during the flow test at which images were obtained: 0 (A1 and B1), 20 (A2 and B2), 60 (A3 and B3) and 120 min (A4 and B4).

maximal distribution of the adhesion rate appeared at 10% for –LPS cells, and at 15% for +LPS cells, as shown in Fig. 6A. Using micro-channel no. 5, the maximal distribution of the adhesion rate appeared at 20% for –LPS cells and at 30% for +LPS cells, as shown in Fig. 6B. It is clear that the plaque-forming abilities of macrophages are accelerated by adding LPS to the culture medium. Figure 6C shows distributions for the adhesion rate of plaque-forming macrophages within chip type 3. One hundred micro-pillars within the chip are arranged in the same format as no. 5. The maximal distribution of the adhesion

rate appeared at 5% for –LPS cells, whereas the peak was shifted to 8% for +LPS cells.

Average and SD values of adhesion rate for –LPS and +LPS cells within a variety of channels are summarized in Table 2. The observational pillar number of the type 1 and 2 chip is twenty ($n = 20$). Channel no. 5 in the type 1 chip showed the largest difference between –LPS and +LPS cells. The average value for the adhesion rate was $14.1 \pm 6.6\%$ for –LPS cells and $25.4 \pm 8.1\%$ for +LPS cells. When –LPS cells went into channel no. 1–3, there was no clear difference between –LPS and +LPS cells. Since

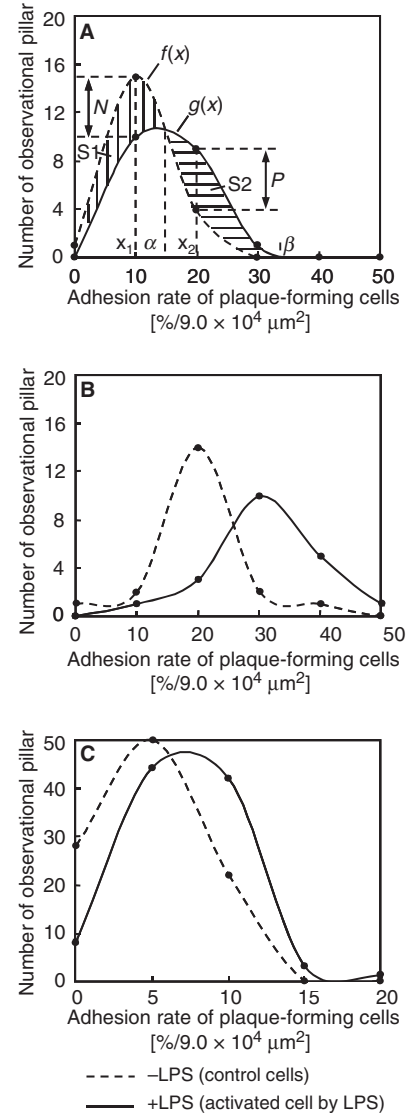


Fig. 6. Distributions for an adhesion rate of plaque-forming macrophages. (A,B): a micro-channel chip (type 1 as shown in Table 1) was used. Each set of data corresponds to the cells throughout micro-channel no. 4 (A) and no. 5 (B), respectively. Number of observational pillars (N): $n = 20$. (C) A micro-channel chip (type 3 as shown in Table 1) was used; $n = 100$. Symbols in (A): $f(x)$ and $g(x)$, general expression for distributions; $S1$ and $S2$, area under the curve; α and β , coordinate points; x_1 and x_2 , coordinate points; N and P , difference between $f(x)$ and $g(x)$.

micro-pillars were arranged in a rectangular pattern within a channel, the flow of cells was disrupted between pillars and the analysis of plaques was difficult.

Table 2. Adhesion rate of plaque-forming macrophages

Chip	Micro-channel no.	Adhesion rate of –without LPS		Adhesion rate of + with LPS		Effectiveness parameter		
		Average (%/9.0 × 10 ⁴ μm ²)	SD (%)	Average (%/9.0 × 10 ⁴ μm ²)	SD (%)	N ^c	P ^c	D
Type 1 ^a	1	4.7	± 5.0	10.6	± 9.1	–8	4	32
	2	7.6	± 6.5	12.9	± 10.1	–7	4	28
	3	8.6	± 6.8	8.6	± 5.2	5	–1	5
	4	6.5	± 4.1	10.3	± 4.9	–5	5	25
	5	14.1	± 6.6	25.4	± 8.1	–11	8	88
Type 2 ^a	1	0		0		0	0	0
	2	6.1	± 4.6	9.4	± 10.2	–4	1	4
	3	2.2	± 2.4	6.9	± 4.0	0	4	0
	4	3.8	± 4.8	none ^b	—	—	—	—
	5	2.2	± 1.6	none ^b	—	—	—	—
Type 3 ^a	1–5	3.0	± 2.0	5.1	± 3.9	–20	20	400

^aSee Table 1.

^bImpossible to measure.

^cSee equation (5) and (6).

There was no adhesion of –LPS or +LPS cells to the channel wall within channel no. 1 in the type 2 chip, where no micro-pillars were arranged within the channel. This result suggests that the arrangement of micro-pillars in a micro-channel is important in determining the adhesion field of flowing cells. With channel no. 4 and 5 in the type 2 chip, micro-pillars were crowded within the channel. In these channels, was difficult to maintain flow of +LPS cells in solution because the channel gradually became blocked during the flow test, suggesting that when micro-pillars are crowded into a narrow space, channel blocking is promoted.

Evaluation of plaque formation by macrophages

Figure 6A shows an analysis procedure for evaluation of plaque formation. Here, the distribution curve of the number of observational pillars (n for –LPS and +LPS cells) is a function of the adhesion rate, x . Two distributions can be expressed as $f(x)$ and $g(x)$, respectively. Changes in the two distributions can be defined by the following two equations, equations 2 and 3:

$$\int_0^{\alpha} \{f(x) - g(x)\} dx = S1 \quad (2)$$

and

$$\int_{\alpha}^{\beta} \{g(x) - f(x)\} dx = S2 \quad (3)$$

where S1 and S2 are the area of the curve, and α and β are coordinate points.

If n (the number of two functions) is equal, the following equation 4 has equality:

$$S1 = S2. \quad (4)$$

A coordinate point giving rise to a maximal increase or decrease for S1 and S2 is shown as x_1 and x_2 , respectively, in Fig. 6A. The differences between two functions at the coordination of x_1 and x_2 can be defined as follows:

$$N = f(x_1) - g(x_1) \quad (5)$$

$$P = g(x_2) - f(x_2). \quad (6)$$

Therefore, changes in two functions are correlated with a change in N and P values, as showing in Fig. 6A. Here, the rate of changes between two functions is defined as in the following equation 7:

$$D = |N \times P|, \quad (7)$$

where D is an effectiveness parameter for two distributions.

The effectiveness parameter evaluated by equation 7 is summarized in Table 2. Micro-channel no. 5 ($n = 20$) in the type 1 chip showed the largest value of D at 88, as well as the largest changes in plaque formation by LPS addition. Four other channels had low values. The arrangements of no. 1–4 micro-channels of micro-pillars were

ineffective for comparing plaque formation of –LPS and +LPS cells. The type 3 chip arranged with channel no. 5 from the type 1 chip showed a D value of 400. This chip had 100 micro-pillars, as well as $n = 100$, meaning that differences between the distribution rates of –LPS and +LPS cells were very large.

Discussion

In the present study, fluid resistance in a micro-channel could be controlled by the arrangement of micro-pillars within the micro-channel. Our preliminary experimental results have confirmed that mobility distributions of particles within micro-channel no. 1 appeared at 2×10^3 to 6×10^3 μm/s, whereas the distribution decreased to a range of 1×10^3 to 2×10^3 μm/s within micro-channel no. 5. It was confirmed that meandering flow was generated in a micro-channel when the arrangement of micro-pillars was in a zigzag formation. Therefore, average flow rate in a micro-channel where micro-pillars were arranged in such a zigzag formation was reduced to 50% compared with that of a micro-channel with micro-pillars arranged in a linear formation.

Simulation of cell adhesion to bioactive surfaces has been reported (10). Leukocyte adhesion during flow in the microvasculature is known to be a multistep process. These interactions

are mediated by binding between receptors on the leukocyte surface and complementary ligands on the surface of endothelial cells. Compared with the results of previous studies, our results suggest that macrophages which have adhered to the surface of a micro-pillar are physically attached.

We established a production method in which projections are arranged within a micro-channel coated with a silicon rubber layer and found that there was no adhesion of macrophages when the micro-channel was not coated in silicon rubber. Thus, we examined the effectiveness of micro-pillars as a trapping technique for cell adhesion in a fluid.

In the present study, we confirmed that LPS-activated macrophages adhere easily after a short experimental time in a rapidly flowing liquid stream (Fig. 6B). In addition, the remarkable increase of the average adhesion rate of LPS-activated macrophages suggests that a possible mechanism of plaque formation by macrophages takes place in two steps, namely: (1) the LPS-activated macrophages physically adhere to a silicon rubber layer on micro-pillars; and (2) cells further adhere to the activated macrophage layer, as well as to the adhesion layer.

Recently, it was reported that periodontopathic bacterial LPS acts as a reservoir for medically important virulence factors that cause systemic disorders (11). In addition, macrophages were found to play a crucial role in the development of atherosclerosis, especially in the initial accumulation of LDL during the progression of lesions to advanced plaques (12). Qi *et al.* (2) have reported that, as well as *A. ac-*

tinomycescomitans, *P. gingivalis* (the major pathogen in periodontitis) was detected in human atheromatosis. This finding suggests that periodontopathic bacterial infection may be associated with atherosclerosis. If a micro-channel chip is further developed, it will be useful tool for analysis of plaque formation within blood vessels.

In conclusion, it was possible to control fluid resistance in a micro-channel by altering the arrangement of micro-pillars within that micro-channel. When there is a low liquid flow rate in a micro-channel, LPS-activated macrophages and control macrophages tend to adhere on side walls of micro-pillars within the micro-channel. Further, LPS-activated macrophages adhered within a short experimental time in rapidly flowing liquid streams.

Acknowledgements

This work was supported by funds from the Project to Develop 'Innovative Seeds' for Japan Science and Technology Agency.

References

1. Nakano K, Inaba H, Nomura R *et al.* Detection and serotype distribution of *Actinobacillus actinomycetemcomitans* in cardiovascular specimens from Japanese patients. *Oral Microbiol Immunol* 2007;**22**: 136–139.
2. Qi M, Miyakawa H, Kuramitsu HK. *Porphyromonas gingivalis* induces murine macrophage foam cell formation. *Microb Pathog* 2003;**35**:259–267.
3. Lakio L, Lehto M, Tuomainen AM *et al.* Pro-atherogenic properties of lipopolysaccharide from the periodontal pathogen

Actinobacillus actinomycetemcomitans. *J Endotoxin Res* 2006;**12**:57–64.

4. Pussinen PJ, Vilkkuna-Rautiainen T, Alfthan G *et al.* Severe periodontitis enhances macrophage activation via increased serum lipopolysaccharide. *Arterioscler Thromb Vasc Biol* 2004;**24**:2174–2180.
5. Baranova I, Vishnyakova T, Bocharov A *et al.* Lipopolysaccharide down regulates both scavenger receptor B1 and ATP binding cassette transporter A1 in RAW cells. *Infect Immun* 2002;**70**:2995–3003.
6. Groeneweg M, Kanters E, Vergouwe MN *et al.* Lipopolysaccharide-induced gene expression in murine macrophages is enhanced by prior exposure to oxLDL. *J Lipid Res* 2006;**47**:2259–2267.
7. Nishihara T, Ohsaki Y, Ueda N, Saito N, Mundy GR. Mouse interleukin-1 receptor antagonist induced by *Actinobacillus actinomycetemcomitans* lipopolysaccharide blocks the effects of interleukin-1 on bone resorption and osteoclast-like cell formation. *Infect Immun* 1994;**62**:390–397.
8. Nishihara T, Ishihara Y, Noguchi T, Koga T. Membrane IL-1 induces bone resorption in organ culture. *J Immunol* 1989;**143**: 1881–1886.
9. Nishihara T, Fujiwara T, Koga T, Hamada S. Chemical composition and immunobiological properties of lipopolysaccharide and lipid-associated proteoglycan from *Actinobacillus actinomycetemcomitans*. *J Periodont Res* 1986;**21**:521–530.
10. Tees DFJ, Chang KC, Rodgers SD, Hammer DA. Simulation of cell adhesion to bioactive surfaces in shear: the effect of cell size. *Ind Eng Chem Res* 2002; **41**:486–493.
11. Nishihara T, Koseki T. Microbial etiology of periodontitis. *Periodontol* 2000 2004; **36**:14–26.
12. Murakami T, Yamada N. Modification of macrophage function and effects on atherosclerosis. *Curr Opin Lipidol* 1996; **7**:320–323.

This document is a scanned copy of a printed document. No warranty is given about the accuracy of the copy. Users should refer to the original published version of the material.